PROCEEDINGS OF SCIENCE

Time Domain Astronomy with *Swift* and *Fermi*

Neil Gehrels*
Astroparticle Physics Division, NASA/Goddard Space Flight Center, Greenbelt, MD 20771, USA
E-mail: neil.gehrels@nasa.gov

John K. Cannizzo
CRESST/Joint Center for Astrophysics, Univ. of Maryland, Baltimore County, Baltimore, MD 21250, USA
E-mail: john.k.cannizzo@nasa.gov

Swift and *Fermi* are unveiling an unexpectedly rich tapestry of behavior in the transient γ−ray sky. Sources which were already known to be transient − such as pulsars, gamma-ray bursts, and blazars − have been studied in ever-increasing detail. For example, *Fermi*/LAT has detected 117 pulsars of which 56 are new. Many of them are only seen so far in γ−rays. In the last $\sim$5 years the Crab Nebula, long taken to be a standard candle, has been observed to flare dramatically. A long monitoring campaign on Sgr A* with *Swift* has shown multiple flares on time scales of tens of days. Other sources not usually associated with high-energy emission − e.g., novae and flare stars − are proving to be interesting at γ−ray energies. Discoveries have been made of spectacular transient emission from tidal disruption events and supernova shock breakout. We present an overview of recent γ−ray and hard X-ray observations and discuss their impact on high-energy astrophysics.

10th INTEGRAL Workshop: "A Synergistic View of the High Energy Sky" - Integral2014,
15-19 September 2014
Annapolis, MD, USA

*Speaker.

PoS(Integral2014)005

1. Background

Historically, astronomers have come to associate $\gamma-$ray emission[1] with objects whose surfaces lie in a deep potential well, i.e., $\varepsilon \equiv GM/(Rc^2) \gtrsim 0.1$, and are therefore able either to launch powerful jets or to heat optically thin gas to a high virial temperature $T_{\rm vir} \simeq (m_p c^2/k_B)\varepsilon \simeq 94$ MeV, for $\varepsilon \simeq 0.1$. This limits the list of potential candidates to neutron stars (NSs) and black holes (BHs). For example, *Swift* (Gehrels et al. 2004) routinely monitors galactic BH transients like GRO 1655-40 as strong, persistent sources, and flares from blazars such as PKS 2155-304 are frequently observed by HESS, an atmospheric Cherenkov telescope array, at energies above 300 GeV.

Somewhat unexpectedly, the last few years have witnessed an explosion in detections of $\gamma-$ray emission from novae and flare stars. This is a little surprising given the standard viewpoint, which stems from the fact that $\varepsilon \simeq 3\times10^{-4}$ for a white dwarf (WD) and $\sim 2\times10^{-6}$ for a $1M_\odot$ main sequence star. Hence such detections strongly indicate nonthermal emission mechanisms at work, such as synchrotron or inverse Compton processes occurring within colliding winds, or internal shocks within an expanding outflow.

2. Gamma Ray Pulsars

Fermi (Atwood et al. 2009) has detected many new $\gamma-$ray pulsars (Abdo et al. 2013), some of which have subsequently turned up in the radio, and some of which are so far only seen in $\gamma-$rays. Abdo et al. (2013) discuss and categorize the 117 *Fermi* $\gamma-$ray pulsars detected up to that time: 61 were known in radio and/or X-rays before *Fermi*; 36 were found in blind searches of *Fermi*/LAT data, and 20 in radio searches of unassociated LAT sources.

3. Crab GeV Flare

For many decades since its detection in X-rays the Crab Nebula has been taken to be a prototypical standard candle. Its power output ultimately derives from the spin-down energy of the Crab pulsar, which is a manifestly stable flywheel. The spin-down power $\dot{E}_{\rm loss} = I\Omega\dot{\Omega}$ where I is the neutron star moment of inertia and Ω the rotational rate ($\sim$30 Hz). Evaluating the loss rate assuming neutron star parameters $M = 1.4M_\odot$, $R = 12$ km, and $I = 1.4\times10^{45}$ g cm^2 yields $\dot{E}_{\rm loss} = 6.4\times10^{38}$ erg s^{-1}, in line with the total nebula power output. Based on these simple considerations, the recent finding of large GeV flares coming from the Crab nebula was totally unexpected. These flares (Figure 1) have been seen with *AGILE* (Tavani et al. 2011) and by *Fermi*/LAT (Abdo et al. 2011). The synchrotron nebula increased and then decreased its power output by a factor $\sim$30 over an observation of several weeks. During these high-energy observations there was also low energy coverage from *Chandra*, *Swift*, *RXTE*, and *MAXI*. Little or no variability was seen at other wavelengths.

At the smallest temporal resolution of the observations, the $\sim$1 hr variability timescales imply a $\sim$milliarcsec scale at the distance of the Crab. The luminosity of the brightest flare was $\sim10^{39}$ erg s^{-1}. It may be that the flares are due to magnetic reconnection in small knots within the nebula, and therefore represent localized but large perturbations to the overall energy budget.

[1]This does not include extended emission, such as that due to radioactive decay of ^{26}Al along the galactic plane.

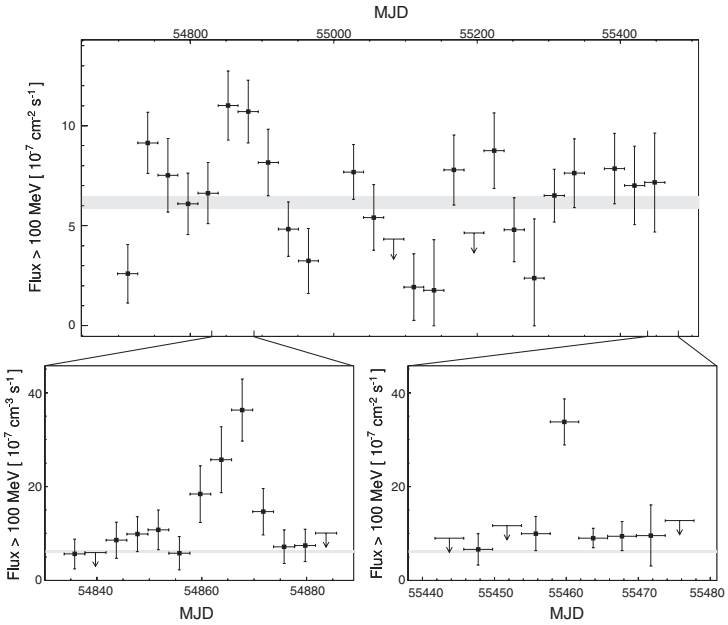

Figure 1: A light curve of the Crab nebula for photons with $E > 100$ MeV as observed by *Fermi*/LAT (Abdo et al. 2011).

4. Galactic Transient – V407 Cyg

V407 Cyg is a binary consisting of a Mira-type pulsating red giant (RG) with a WD companion. The 745-day pulsation period of the RG in conjunction with the Mira period-luminosity relation gives a distance $D \simeq 2.7$ kpc. On 10 March 2010 a nova outburst was detected from V407 Cyg. Abdo et al. (2010) report subsequent detections in *Fermi*/LAT at energies above 100 MeV (Figure 2). They argue this emission arises from the nova shell in a dense environment.

They examine two scenarios, one in which π^0 decay dominates, and another involving inverse Compton scattering. The time scale for pp interactions in the π^0 decay model is $t_{\rm pp} \simeq 1/[4n(R)c\sigma_{\rm pp}] \simeq 32$ d, where $n(R)$ is the adopted radial CSM density law. The pp cross section $\sigma_{\rm pp} \simeq 3 \times 10^{-26}$ cm^2. Hence $t/t_{\rm pp} \sim 3\%$ of the protons can interact to produce π^0 emission on a 1 d time scale. In the inverse Compton (IC) model the cooling time scale for electrons with $E_e \simeq 5$ GeV capable of upscattering $\sim$3000 K photons to $\sim$100 MeV is $t_{\rm IC} = (3/4)m_e^2c^3[\sigma_T E_e u_{\rm IR}(R)]^{-1} \simeq 3.6$ d, where $u_{\rm IR}(R)$ characterizes the radial dependence of the IR radiation energy density and σ_T is the Thomson electron scattering cross section. Hence $t/t_{\rm IC} \sim 28\%$ of the electrons produce $\gamma-$ radiation efficiently in $\sim$1 d. Abdo et al. (2010) test both models against observations and conclude that both are consistent with the data. The Fermi-LAT detection of V407 Cyg was a surprise and adds novae to the list of transient $\gamma-$ray emitters. As of now we have *Fermi*/LAT light curves for four novae (Ackermann et al. 2014).

5. GRBs

GRBs come in two kinds, long and short, where the dividing line between the two is $\sim$2 s. A further division can be made spectrally according to their hardness ratio (i.e., ratio of high to low

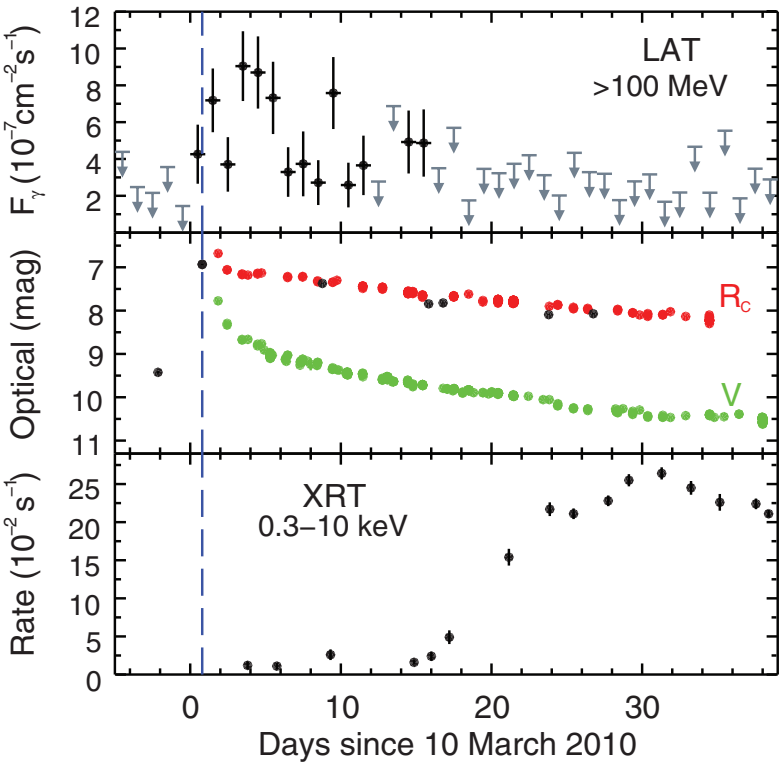

Figure 2: Light curves of V407 Cyg in $\gamma-$rays (Abdo et al. 2010) from *Fermi*/LAT (*upper panel*), optical (*middle panel*), and X-rays as seen by *Swift*/XRT (*bottom panel*). Vertical dashed blue line indicates the time of the optical nova. The $\gamma-$rays peak 3 to 4 d later.

energies). The redshift range is from about 0.2 to 2 for short GRBs (sGRBs), with a mean of about 0.4. For long GRBs (lGRBs) the range is between about 0.009 and 8.2, with a mean of about 2.3. The typical energy release is $\sim 10^{49} - 10^{50}$ erg for sGRBs and $\sim 10^{50} - 10^{51}$ erg for lGRBs. These ranges are based on observed isotropic-equivalent energies of $\sim 10^{51}$ erg for sGRBs and $\sim 10^{53}$ erg for lGRBs, and estimates for jet beaming for each class, $\theta_j \sim 5^\circ$ for lGRBs and $\theta_j \sim 15^\circ$ for sGRBs. Beaming angles for sGRBs are still highly uncertain. The corresponding beaming factors $f_b = 1 - \cos\theta_j \simeq \theta_j^2/2$ are roughly $1/300$ for lGRBs and $1/30$ for sGRBs.

Current theory says that long GRBs are due to the explosion of a massive star, possibly with high angular momentum and perhaps also lower than average metallicity. Short GRBs are thought to be due to merging neutron stars. All long GRBs that are close enough to study in detail optically have been found to have associated type Ic supernovae; in contrast no short GRB has shown a concomitant supernova.

6. High z GRBs and the Metallicity and SFR Histories of the Universe

GRBs are incredibly bright. A typical galaxy at a redshift of only $z = 3$ is fainter than $m \simeq 27$, whereas the optical component of GRB prompt emission (Figure 3), when seen, can be as high as $m \simeq 10 - 15$. For GRBs, the current record holder is GRB 090429B at $z \simeq 9.4$ (Cucchiara et al. 2011). Multiwavelength observations of high z GRBs are providing information about the universe

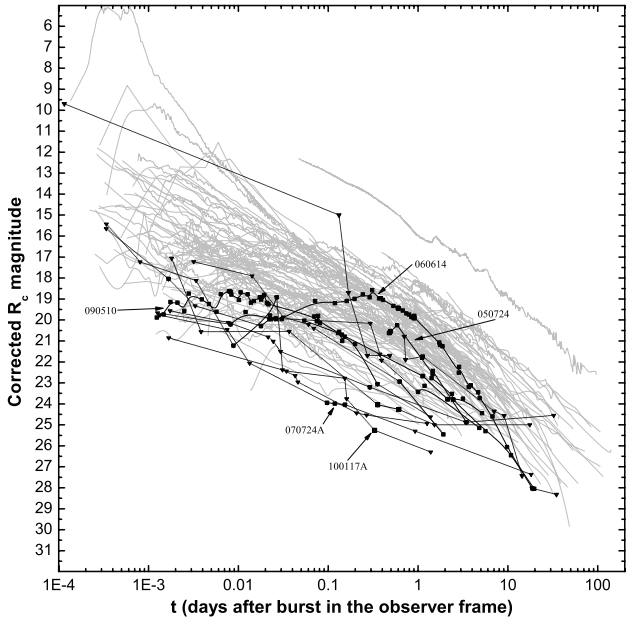

Figure 3: R-band afterglow light curves, corrected for Galactic extinction and host galaxy contribution, of Type I (black lines and points) and Type II (thin gray lines) GRBs (Kann et al. 2011). These types correspond closely to short and long GRBs, respectively. In general the optical afterglows are fainter for short GRBs.

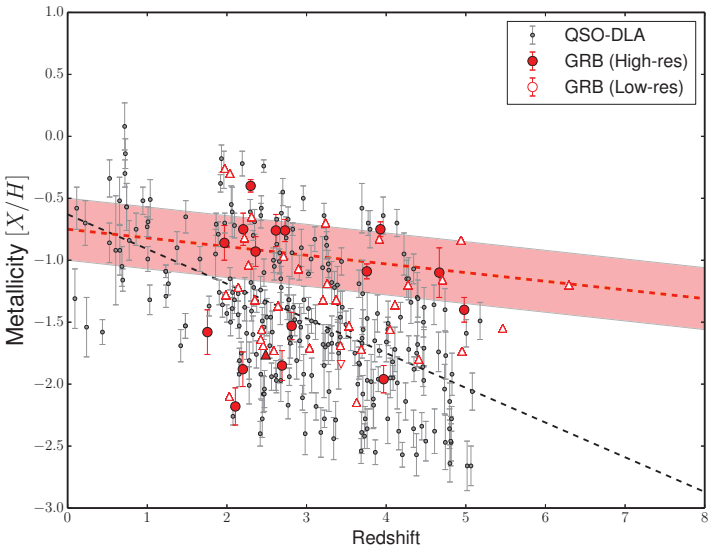

Figure 4: Metallicity versus redshift for QSO-DLA and GRBs (Cucchiara et al. 2014).

at a time when it was only about 4% of its current age, and shed light on the process of reionization in the early universe. Strong absorption lines detected in QSO spectra, damped Lyman$-\alpha$ (DLA) systems, originate in galaxies crossing sight lines. A study of the DLA systems associated with optical spectra of GRBs and their hosts has provided detailed information on the metallicity history of the universe, and allowed a comparison of the metallicity history inferred from similar studies involving QSOs (Figure 4). For instance Savaglio et al. (2006) find that the metallicity for GRBs

on average is ∼5 times larger than in QSOs.

GRBs are also being used to determine the star formation rate to high redshift (Figure 5). Corrections need to be made for systematic effects that alter the proportionality between measured GRB rates and inferred star formation rates, such as possible metallicity bias. The star formation rate from GRBs is higher than from other techniques. GRBs provide a more complete measure of star formation from all types of galaxies.

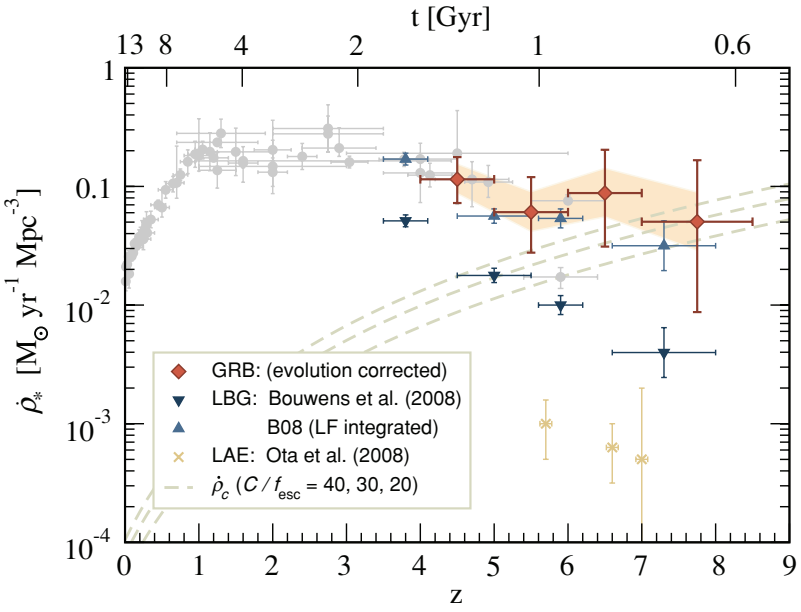

Figure 5: The cosmic star formation rate (SFR) history (Kistler et al. 2009), with data from several sources (Hopkins & Beacom 2006, Bouwens et al. 2008, Ota et al. 2008). The rates inferred from high$-z$ GRBs are shown as diamonds. The three dashed curves (Madau et al. 1999) give the critical SFR $\dot{\rho}_c$ required to balance recombination, for $C/f_{\rm esc} = 40$, 30, and 20 (top to bottom), where C is the clumpiness of the intergalactic medium and $f_{\rm esc}$ the fraction of photons that escape their galaxy.

7. Jetted Tidal Disruption Event SW1644

Tidal disruption events (TDEs) are caused by the tidal disruption of stars that venture too close to the massive black holes (MBHs) at the centers of galaxies (Rees 1988, Phinney 1989). Prior to March 2011, nearly all our observational information was based on optical/UV studies or long-term X-ray data with poor time sampling. This changed with the discovery by *Swift* of GRB 110328A/Swift J1644 (= Sw1644), a TDE viewed down the jet axis of a MBH in the nucleus of a galaxy at redshift $z = 0.35$ (Bloom et al. 2011, Burrows et al. 2011, Levan et al. 2011). Continued observations for over 1 yr with the *Swift*/XRT has shown an apparent long term decay law $L_x \propto t^{\alpha}$ with $\alpha \simeq -1.3$ (Figure 6), which may be consistent with the decay of a freely expanding, advectively dominated slim disk (Cannizzo, Troja, & Lodato 2011). This decay law appears to hold as early as $t \simeq 10$ d, indicating that the conventional dividing point between "stellar fallback" ($L \propto t^{-5/3}$) and "disk accretion" ($L \propto t^{-4/3}$) (Phinney 1989, Cannizzo, Lee, & Goodman 1990)

may have been at $\lesssim 10$ d, indicative of a deeply plunging disruption. This is in contrast to the more probable event where a disruption occurs close to the classical tidal disruption radius, in which case the dividing point would lie at years to decades. If Sw1644 was deeply plunging, that may also be part of the reason it was a powerful, jetted TDE.

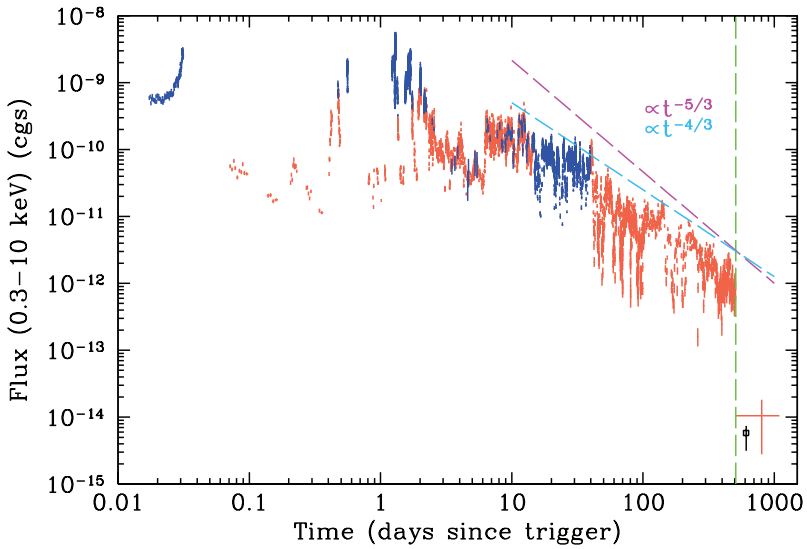

Figure 6: The long term XRT light curve for Swift 1644, the jetted tidal disruption event (Mangano et al. 2014). The decay closely follows -4/3; a decay -5/3 is disfavored.

8. A Superflare from DG CVn

On 23 April 2014 *Swift*/BAT detected a superflare in the dM4e+dM4e flare star binary system DG CVn. It arose from one of the stars in this nearby (18 pc) red dwarf system. Both stars have masses and radii $\sim 1/3$ solar; their orbital separation is ~ 3 AU. The flare consisted of a series of outbursts; the strongest was $\sim 10^4$ times more energetic than the largest solar flare ever seen – the Carrington Event of 1859.

Time resolved spectral fitting implies $T \simeq 2 \times 10^8$ K and $L_X \simeq 1.9 \times 10^{32}$ erg s^{-1} at the peak of the flare. This compares with a normal systemic bolometric luminosity 1.3×10^{32} erg s^{-1}. As with a previous superflare seen in 2008 in EV Lac (Osten et al. 2010), for several minutes the X-ray emission from the flare outshone the total light from the system. The rotational and activity characteristics of DG CVn imply membership in the young star population rather than the dominant Gyr-old thick disk population, making such activity more likely.

9. Sgr A* Flares

The closest and best studied SMBH is of course Sgr A* at ~ 8 kpc, the center of the galaxy. Its bolometric luminosity is lower than expected from an Eddington-limited SMBH of mass $\sim 4 \times 10^6 M_\odot$ by a factor $\sim 10^8 - 10^9$, indicating the heyday of its quasar-like youth is well past. It has

long since depleted its "loss cone" (Frank & Rees 1976) supply of stars and gas for steady accretion, and its accretion is commonly characterized by a radiatively inefficient accretion flow.

Sgr A* emits a steady soft X-ray band luminosity $\sim 2\times10^{33}$ erg s^{-1} (Baganoff et al. 2003) with occasional flaring up by a factor $\sim 5-150$ for tens of minutes to hours. For $\sim$5 yr beginning in 2006, *Swift*/XRT observed a $\sim 21^{'}\times 21^{'}$ region around Sgr A*. Six flares were seen, with luminosities $\sim(1-3)\times10^{35}$ erg s^{-1} (Figure 7). Based on the number of observed flares and the total length of observations, Degenaar et al. (2013) estimate a flaring rate $0.1-0.2$ d^{-1}. This implies a bright flare with $L_X \simeq 10^{35}$ erg s^{-1} occurs every $\sim 5-10$ d. This rate is in accord with previous estimates based on *Chandra* data (Baganoff et al. 2003).

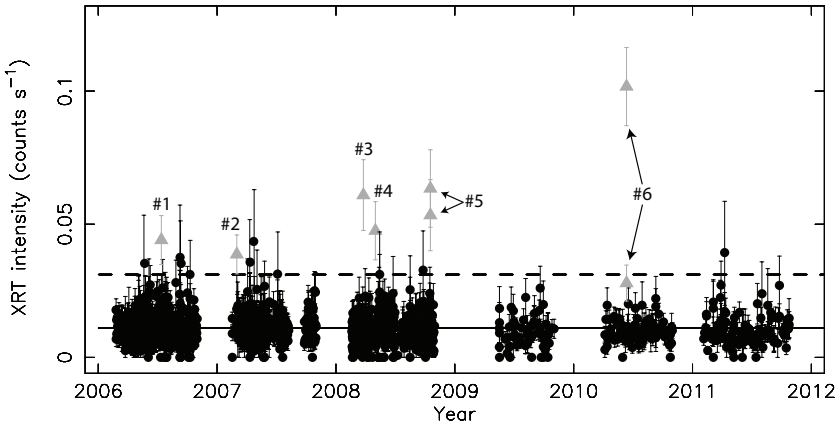

Figure 7: Long term 0.3-10 keV *Swift*/XRT light curve of Sgr A* (Degenaar et al. 2013). There were six confirmed X-ray flares (numbered).

10. SN 2008D Shock Breakout

The $t=0$ time of a SN is marked by a burst of neutrinos, thus the "delayed" optical light from radioactivity in the ejecta through which most SNe are discovered does not provide information about the first moments following the explosion. On 2008 January 9 *Swift*/XRT serendipitously discovered an extremely bright X-ray transient (Figure 8, Soderberg et al. 2008) while undertaking a preplanned observation of the galaxy NGC 2770 ($d=27$ Mpc). Two days earlier *Swift*/XRT had observed the same location and did not see a source. X-ray outburst (XRO) 080109 lasted about 400 s and occurred in one of the galaxy's spiral arms. XRO 080109 was not a GRB (no $\gamma-$rays were detected), and the total X-ray energy $E_X \simeq 2\times10^{46}$ erg was orders of magnitude lower than a GRB. The peak luminosity $\sim 6\times10^{43}$ erg s^{-1} is much greater than the Eddington luminosity for a $\sim 1M_\odot$ object, and also from type I X-ray bursts. Therefore the standard accretion and thermonuclear flash scenarios are excluded.

Simultaneous *Swift*/UVOT observations did not reveal a counterpart, but UVOT observations at 1.4 hr showed a brightening. Gemini North 8-m telescope observations beginning at 1.7 d revealed a spectrum suggestive of a young SN (Soderberg et al. 2008). Later observations confirmed the spectral features. The transient was classified as a type Ibc SN based on the lack of H, and weak Si features.

Soderberg et al. (2008) argue that the X-ray flash indicates a trans-relativistic shock breakout from a SN, where the radius at breakout is $\gtrsim 7 \times 10^{11}$ cm, and the shock velocity at breakout is $\gamma\beta \lesssim 1.1$. Soderberg et al. (2008) estimate a circumstellar density which yields an inferred pre-SN mass loss rate $\sim 10^{-5} M_{\odot}$ yr^{-1}, reinforcing the notion of a Wolf-Rayet progenitor. The similarity between the shock break-out properties of the He-rich SN 2008D and the He-poor GRB-associated SN 2006aj are consistent with a dense stellar wind around a compact Wolf-Rayet progenitor.

X-ray and radio observations presented by Soderberg et al. (2008) of SN 2008D are the earliest ever obtained for a normal type Ibc SN. At $t < 10$ d, the X-ray and peak radio luminosities are orders of magnitude less than those of GRB afterglows, but comparable to those of normal type Ibc SN.

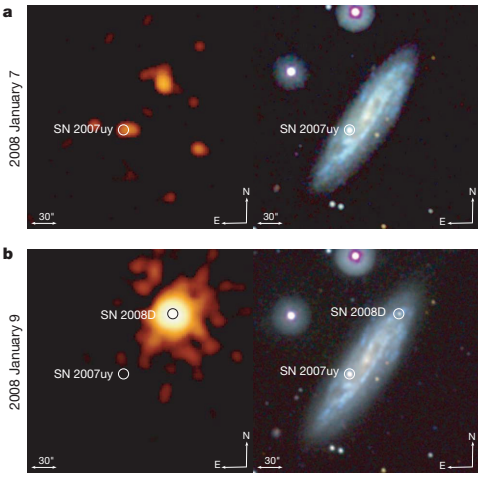

Figure 8: X-ray (left) and optical (right) discovery images for SN2008D (Soderberg et al. 2008).

11. Conclusion

In summary, the sky is rich in transients of many types. This has been known for millenia in the optical, and now, thanks to *Swift*, *Fermi*, and other high-energy observatories, we know it to be true for a wide variety of objects in $\gamma-$rays. *Swift* and *Fermi* are exploring the transient sky with unprecedented sensitivity and coverage, thereby enhancing our understanding of previously known high-energy transient behavior of sources like pulsars and accreting BHs, as well as uncovering new phenomena – high-energy emission from unlikely sources. Every year brings new discoveries

in time domain science. Looking to the future, gravitational wave detections by aLIGO-Virgo will open up new opportunities for joint gravity wave-electromagnetic synergism.

References

[1] Abdo, A. A., et al. 2010, Science, 329, 817

[2] Abdo, A. A., et al. 2011, Science, 331, 739

[3] Abdo, A. A., et al. 2013, ApJS, 208, 17

[4] Ackermann, M., et al. 2014, Science, 345, 554

[5] Atwood, W. B., et al. 2009, ApJ, 697, 1071

[6] Baganoff, F. K., et al. 2003, ApJ, 591, 891

[7] Bloom, J. S., et al., 2011, Science, 333, 203

[8] Bouwens, R. J., Illingworth, G. D., Franx, M., & Ford, H. 2008, ApJ, 686, 230

[9] Burrows, D. N., et al. 2011, Nature, 476, 421

[10] Cannizzo, J. K., Lee, H. M., & Goodman, J. 1990, ApJ, 351, 38

[11] Cannizzo, J. K., Troja, E., & Lodato, G. 2011, ApJ, 742, 32

[12] Cucchiara, A., et al. 2011, ApJ, 736, 7

[13] Cucchiara, A., Fumagalli, M., Rafelski, M., Kocevski, D., Prochaska, J. X., Cooke, R. J., Becker, G. D. 2014, arXiv1408.3578

[14] Degenaar, N., Miller, J. M., Kennea, J., Gehrels, N., Reynolds, M. T., & Wijnands, R. 2013, ApJ, 769, 155

[15] Drake, S., Osten, R., Page, K. L., Kennea, J. A., Oates, S. R., Krimm, H., & Gehrels, N. 2014, ATel, 6121, 1

[16] Frank, J., & Rees, M. J. 1976, MNRAS, 176, 633

[17] Gehrels, N., et al. 2004, ApJ, 611, 1005

[18] Hopkins, A. M., & Beacom, J. F. 2006, ApJ, 651, 142

[19] Kann, D. A., et al. 2011, ApJ, 734, 96

[20] Kistler, M. D., Yüksel, H., Beacom, J. F., Hopkins, A. M., & Wyithe, J. S. B. 2009, ApJ, 705, L104

[21] Levan, A. J., et al. 2011, Science, 333, 199

[22] Madau, P., Haardt, F., & Rees, M. J. 1999, ApJ, 514, 648

[23] Mangano, V., Burrows, D. N., Sbarufatti, B., & Cannizzo, J. K. 2014, ApJ, submitted

[24] Osten, R. A. et al. 2010, ApJ, 721, 785

[25] Ota, K., et al. 2008, ApJ, 677, 12

[26] Phinney, E. S. 1989, in The Center of the Galaxy, ed. M. Morris, 136, 543

[27] Rees, M. J. 1988, Nature, 333, 523

[28] Savaglio, S. 2006, New Jour. Phys., 8, 195

[29] Soderberg, A. M., et al. 2008, Nature, 453, 469

[30] Tavani, M., et al. 2011, Science, 331, 736